www.ietdl.org

Published in IET Optoelectronics
Received on 11th January 2011
Revised on 9th June 2011
doi: 10.1049/iet-opt.2011.0004

ISSN 1751-8768

Engineering method for predicting junction temperatures of high-power light-emitting diodes

X. Luo[1] *Z. Mao*[1] *J. Yang*[2] *S. Liu*[2]

[1]*School of Energy and Power Engineering, Huazhong University of Science and Technology, Wuhan, Hubei 430074, People's Republic of China*
[2]*Wuhan National Lab for Optoelectronics, Huazhong University of Science and Technology, Wuhan, Hubei 430074, People's Republic of China*
E-mail: Luoxb@mail.hust.edu.cn

Abstract: In order to evaluate the reliability of a high-power light-emitting diode (LED) module, it is important to obtain junction temperature of high-power LED modules in various applications. However, until recently, there were no simple and effective methods to obtain the junction temperature of LEDs. In this study, an engineering method to estimate the junction temperature of typical LED packaging modules by using an analytical solution was proposed. Simple experiments were used to help determine boundary conditions for thermal modelling. Simulations for obtaining thermal resistance and junction temperature of LED packaging modules in the same boundary conditions were also carried out by commercial software COMSOL. On comparing the junction temperatures obtained by the two methods, it can be seen that the proposed model is able to estimate junction temperatures well.

1 Introduction

Applications of light-emitting diode (LED) in the versatile lighting fields are expanding because of its advantage of energy saving and other positive characteristics. However, as long as its reliability is a concern, LED cannot be used more broadly, especially in general illumination.

Junction temperature is one of the most critical parameters, which directly affects the reliability of LEDs. When customers wish to purchase high-power LED products, what a products' junction temperature is one of the most frequently asked questions. Although there is a strong need to know, it is still challenging to obtain because LED chips are very small and packaged inside the module. Nowadays, researchers [1–4] have proposed various methods to measure junction temperature of an LED module, such as spectrometry and resistance-temperature methods. All of these existing methods calculate the junction temperature by using measuring LED emission wavelengths or voltage across the LED. These measurement steps are complex and the voltage measurement method, for instance, requires very expensive equipment and needs professional engineers for operation. These disadvantages will seriously hinder wider applications of such methods in the industry as whole.

Compared to measuring experiments, simulation is flexible and convenient. It is widely used for analysing the temperature field of LED modules [5]. However, in order to use simulations as a method, professional knowledge of modelling and simulations is needed. Moreover, the accuracy of simulation results is determined by the prescription of simulation boundary conditions. This step still poses problems for engineers when estimating the junction temperature of an LED module.

Thermal modelling method, generally employing analytical solutions, is a widely used method in microelectronic industry for its low cost and accuracy. Bar-Cohen *et al.* [6] proposed a thermal resistance network model to calculate junction temperatures. The network topology is star-shaped and only under isothermal condition can it predict the junction temperature accurately. Rosten *et al.* [7] and Lasance *et al.* [8, 9] established an improved star-shaped compact thermal resistance network model that was boundary condition independent. Surface-to-surface resistors were added to the improved star-shaped network for representing the realistic characterisation of heat transfer in a better manner. In all of the 38 kinds of different conditions mentioned in [9], the improved model can predict the junction temperature accurately; the error is only 1–2%.

Spreading thermal resistance, which appears when heat conducts into a large body from a small area, is the key resistance of thermal modelling. It is common in microelectronics, as well as in LED applications. Many researchers studied spreading thermal resistance in different conditions. Kennedy [10] found analytical solutions of spreading thermal resistance in a cylinder with a constant heat flux over a part of one end and a variety of boundary conditions at the other surfaces. Kadambi and Abuaf [11] and Krane [12] obtained analytical solutions of spreading resistance in two- and three-dimensional (3D) rectangular bodies with insulated sides and a convective boundary condition on the surface opposite to the heat input.

Muzychka *et al.* [13–15] studied spreading thermal resistance widely from a variety of aspects, including heat source location, boundary conditions and types of flux channel and provided a series of analytical expressions for spreading thermal resistance calculation. The present authors [16–19] extended the spreading thermal resistance model and analysed the thermal performance of various packaging including LED applications.

In this paper, an analytical thermal model was proposed for estimating junction temperature. Since LED modules can be used in various application situations, the junction temperature will be different for the same LED module if the heat sink is different. This proposes another problem for application engineers, who usually are optical engineers and are not familiar with heat transfer. To solve the problem, the present analytical thermal model uses an equivalent convective boundary condition to eliminate the effects of different application situations. The equivalent convective boundary condition was accurately achieved through a simple experiment. To understand the feasibility of the thermal model, a numerical simulation was also used to estimate the junction temperature. A comparison of the simulation results and analytical results shows that the present engineering method can be used for predicting the junction temperature.

2 Thermal modelling of an LED module

Fig. 1*a* shows a general LED lighting application. In the application, an LED module is mounted on an MCPCB for electrical connection. The MCPCB is placed on a heat sink with a thermal interfacial material (TIM) layer to cool the LED module. According to the structure shown in Fig. 1*a*, heat generated by the LED module flows through the MCPCB layer, TIM layer and heat sink, respectively, and finally dissipates into ambient. To simplify thermal analysis of the heat transfer processes, an equivalent heat transfer coefficient h_{equ}, as shown in Fig. 1*b*, is loaded at the bottom surface of the LED module to stimulate the cooling effect brought by the MCPCB layer, TIM layer and heat sink. Determination of the equivalent heat transfer coefficient will be given in the following. Therefore thermal modelling of an LED lighting application can be focused on an LED module.

Fig. 2 is a section of a typical LED module, which is comprised of an LED chip, a TIM layer, an aluminium stage, a copper heat sink, silicone, a PC lens and a moulding compound. When the LED module lights up, heat is generated from the LED chip. Since the top part of the LED module comprises of the silicone and PC lens with low thermal conductivity, only a very small amount of the

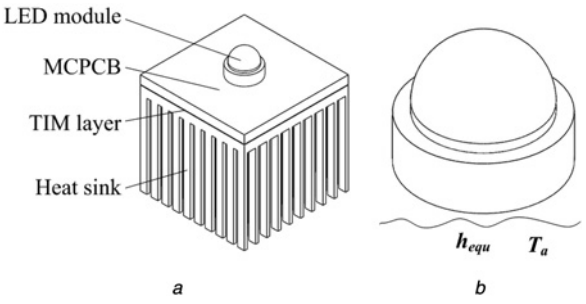

Fig. 1 *LED lighting application and LED module*

a General LED lighting application
b Thermal simplification for LED module

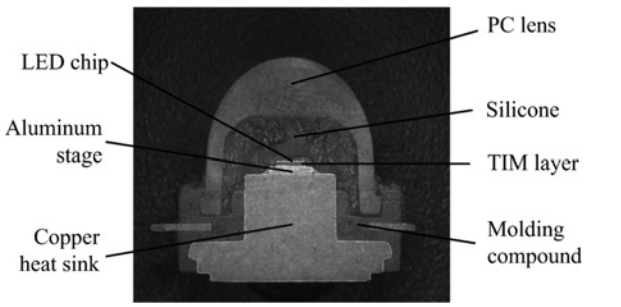

Fig. 2 *Photo of a typical LED module section zoomed in 30 times*

heat dissipates through those parts. Similarly, little heat transfers to ambient through the moulding compound from its surface because of its low thermal conductivity and poor cooling condition. Thus, heat dissipation through the silicone, PC lens and moulding compound can be neglected. In this thermal modelling, it is considered that heat generated by the LED chip only conducts through the layers mainly in a direction perpendicular to the bottom surface of the copper heat sink, as shown in Fig. 3*b*. Based on the heat flow path shown in Fig. 3*b*, a thermal resistance network can be established as in Fig. 3*c*. In the network, R_{TIM}, R_{alu} and R_{cop} are the thermal resistances of TIM layer, aluminium stage and copper heat sink, respectively. Here, temperature at bottom surface of LED chip is considered as junction temperature T_j. $\overline{T_L}$ is the mean temperature of the bottom surface of the copper heat sink.

As shown in Fig. 3*a*, the TIM layer is smaller than the aluminium stage, which is also much smaller than the copper heat sink. When heat is conducted from the TIM to the aluminium stage or from the aluminium stage to the copper heat sink, there are spreading thermal resistances that comprise major portions of R_{alu} and R_{cop}. Muzychka *et al.* [15] studied spreading thermal resistance in isotropic flux channels with rectangular heat source and isotropic discs with a circular heat source. The expressions for calculating spreading thermal resistance of the two systems were obtained. In both systems, all of the surfaces, except the bottom surfaces, are adiabatic; the lower surfaces are convective cooling surfaces with a heat transfer coefficient. To use the expressions in [15] to calculate the R_{alu} and R_{cop}, equivalent heat transfer coefficient at the bottom surface should be found, which is equal to the actual heat conduction in the structure as shown in Fig. 3*a*. For instance, in the aluminium stage, an equivalent heat transfer coefficient at the bottom surface used for substituting the actual thermal conduction is obtained as follows. The heat

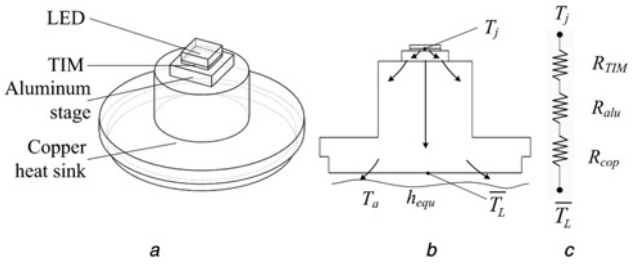

Fig. 3 *Thermal model ling, it is considered that heat generated by the LED chip only conducts through the layers mainly in a direction perpendicular to bottom surface of the copper heat sink*

a Thermal model
b Heat flow path
c Thermal resistances network

dissipation rate for the equivalent heat transfer coefficient is given by

$$Q = h_{\text{equa}} A_{\text{alu}} (\overline{T}_{\text{alu}} - T_{\text{a}}) \tag{1}$$

where h_{equa} is the equivalent heat transfer coefficient at the bottom surface of the aluminium stage, A_{alu} is the area of aluminium stage at the bottom surface, $\overline{T}_{\text{alu}}$ is the mean temperature of the bottom surface and T_{a} is the ambient temperature. From the thermal resistance network, the actual heat dissipation rate is

$$Q = \frac{\overline{T}_{\text{alu}} - T_{\text{a}}}{R_{\text{cop}} + R_{\text{h}}} \tag{2}$$

where R_{h} is the thermal resistance caused by the equivalent heat transfer coefficient h_{equ} loaded at the bottom surface of the LED module. R_{h} is given by

$$R_{\text{h}} = \frac{1}{h_{\text{equ}}(\pi D_3^2/4)} \tag{3}$$

h_{equa} will be obtained by the summary of (1)–(3) and is expressed as

$$h_{\text{equa}} = \frac{1}{(R_{\text{cop}} + R_{\text{h}})A_{\text{alu}}} \tag{4}$$

2.1 Calculation of R_{TIM}

R_{TIM} is the 1D bulk thermal resistance of TIM. According to the dimensions as shown in Fig. 4, R_{TIM} is given by

$$R_{\text{TIM}} = \frac{t_{\text{TIM}}}{k_{\text{TIM}} ab} \tag{5}$$

where k_{TIM} is the thermal conductivity of TIM.

2.2 Calculation of R_{cop}

As shown in Fig. 4, the copper heat sink is divided into three discs to conveniently calculate thermal resistance R_{cop}. Since D_3 is nearly equal to D_2, the occurrence of thermal restriction as heat flows from disc 2 to disc 3 can be ignored. Therefore the thermal resistance of disc 3 can be calculated by 1D thermal conduction resistance and is given as

$$R_3 = \frac{t_3}{k_{\text{cop}}(\pi D_3^2/4)} \tag{6}$$

where k_{cop} is the thermal conductivity of copper.

Spreading thermal resistance also exists when heat is conducted from disc 2 to disc 3. Spreading thermal resistance of disc 2 is calculated using the following expression [15], which depicts the explicit relationship with the geometry of the structure, according to the notion in Fig. 4.

$$R_{2s} = \frac{4}{\pi\varepsilon_2 k_{\text{cop}} D_1} \sum_{n=1}^{\infty} A_{n\_2}(n, \varepsilon_2) B_{n\_2}(n, \tau_2) \frac{J_1(\delta_n \varepsilon_2)}{\delta_n \varepsilon_2} \tag{7}$$

with

$$A_{n\_2} = -\frac{2\varepsilon_2 J_1(\delta_n \varepsilon_2)}{\delta_n^2 J_0^2(\delta_n)} \tag{8}$$

and

$$B_{n\_2} = -\frac{\delta_n + B_{i\_2} \tanh(\delta_n \tau_2)}{\delta_n \tanh(\delta_n \tau_2) + B_{i\_2}} \tag{9}$$

The eigenvalues δ_n are solutions to $J_1(\delta_n) = 0$ and $B_{i\_2} = h_{\text{equ2}} D_2 / 2k_{\text{cop}}$, $\tau_2 = 2t_2/D_2$ and $\varepsilon_2 = D_1/D_2$. h_{equ2} is the equivalent heat transfer at the bottom surface of disc 2. According to (4), h_{equ2} is obtained as

$$h_{\text{equ2}} = \frac{1}{(R_{\text{h}} + R_3)(\pi D_2^2/4)} \tag{10}$$

Since R_2 is the sum of R_{2s} and 1D thermal conduction resistance of disc 2, R_2 is given as

$$R_2 = R_{2s} + \frac{t_2}{k_{\text{cop}}(\pi D_2^2/4)} \tag{11}$$

As the aluminium stage is a rectangular plate, it is necessary to transform the rectangular plate into a circular one by applying the method of geometric equivalence between the rectangular flux channel and the circular flux tube. The following is the rule of transformation

$$D_a = 2\sqrt{\text{cd}/\pi} \tag{12}$$

After geometric equivalence, spreading thermal resistance of disc 1 is calculated as (7), but some parameters are substituted, and given by

$$R_{1s} = \frac{4}{\pi\varepsilon_1 k_{\text{cop}} D_a} \sum_{n=1}^{\infty} A_{n\_1}(n, \varepsilon_1) B_{n\_1}(n, \tau_1) \frac{J_1(\delta_n \varepsilon_1)}{\delta_n \varepsilon_1} \tag{13}$$

where

$$A_{n\_1} = -\frac{2\varepsilon_1 J_1(\delta_n \varepsilon_1)}{\delta_n^2 J_0^2(\delta_n)} \tag{14}$$

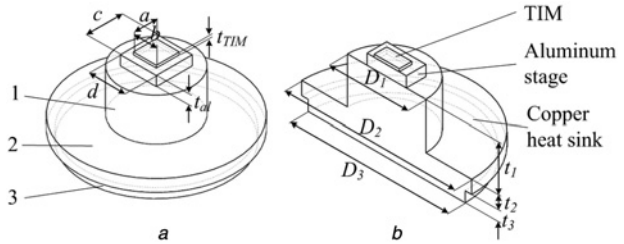

Fig. 4 *Structure dimensions*
a 3D view
b Half-3D view

doi: 10.1049/iet-opt.2011.0004

and

$$B_{n\_1} = -\frac{\delta_n + B_{i\_1}\tanh(\delta_n\tau_1)}{\delta_n\tanh(\delta_n\tau_1) + B_{i\_1}} \tag{15}$$

The eigenvalues δ_n are solutions to $J_1(\delta_n) = 0$ and $B_{i\_1} = h_{\text{equ1}}D_1/2k_{\text{cop}}$, $\tau_1 = 2t_1/D_1$ and $\varepsilon_1 = D_a/D_2$. h_{equ1} is the equivalent heat transfer at the bottom surface of disc 1. It is given as

$$h_{\text{equ1}} = \frac{1}{(R_h + R_3 + R_2)(\pi D_1^2/4)} \tag{16}$$

Similar to R_2, R_1 is given by

$$R_1 = R_{1s} + \frac{t_1}{k_{\text{cop}}(\pi D_1^2/4)} \tag{17}$$

R_{cop} is the sum of thermal resistances of discs 1, 2 and 3. It is obtained as

$$R_{\text{cop}} = R_1 + R_2 + R_3 \tag{18}$$

2.3 Calculation of R_{alu}

Spreading thermal resistance of the aluminium stage can be calculated according to the notions in Fig. 4. The expression [15] is

$$\begin{aligned} R_{\text{als}} = {} & \frac{8}{a^2\text{cdk}_{\text{alu}}}\sum_{m=1}^{\infty}\frac{\sin^2(a/2\delta_m)}{\delta_m^3}\phi(\delta_m) \\ & + \frac{8}{b^2\text{cdk}_{\text{alu}}}\sum_{n=1}^{\infty}\frac{\sin^2(b/2\lambda_n)}{\lambda_n^3}\phi(\lambda_n) \\ & + \frac{64}{a^2b^2\text{cdk}_{\text{alu}}}\sum_{m=1}^{\infty}\sum_{n=1}^{\infty}\frac{\sin^2(a/2\delta_m)\sin^2(b\lambda_n)}{\delta_m^2\lambda_n^2\beta_{m,n}}\phi(\beta_{m,n}) \end{aligned} \tag{19}$$

where

$$\phi(\sigma) = \frac{(e^{2\sigma t_{\text{alu}}} + 1)\sigma - (1 - e^{2\sigma t_{\text{alu}}})h_{\text{equa}}/k_{\text{alu}}}{(e^{2\sigma t_{\text{alu}}} - 1)\sigma + (1 + e^{2\sigma t_{\text{alu}}})h_{\text{equa}}/k_{\text{alu}}} \tag{20}$$

σ is replaced by λ_n, δ_m and $\beta_{m,n}$, accordingly. $\delta_m = 2m\pi/c$, $\lambda_n = 2n\pi/d$ and $\beta_{m,n} = \sqrt{\delta_m^2 + \lambda_n^2}$. k_{alu} is the thermal conductivity of aluminium.

R_{alu} is given by

$$R_{\text{alu}} = R_{\text{als}} + \frac{t_{\text{alu}}}{k_{\text{alu}}\text{cd}} \tag{21}$$

The total thermal resistance of the structure is

$$R_{\text{total}} = R_{\text{TIM}} + R_{\text{alu}} + R_{\text{cop}} \tag{22}$$

Since the total thermal resistance has been obtained, the difference in temperature between bottom surfaces of the LED chip and the structure shown in Fig. 3 is given by

$$\theta = Q_{\text{h}}R_{\text{total}} \tag{23}$$

where Q_{h} is the heat generation rate of the LED chip.

The junction temperature is finally obtained as

$$T_j = \theta + \overline{T}_L \tag{24}$$

It should be noted that the temperature in (24) is the mean value of the bottom surface of the chip and the packaging module. As both bottom surface of the LED chip and the module are very small, the mean temperatures are nearly equal to the real temperature.

3 Determination of equivalent heat transfer coefficient h_{equ}

For the substituted heat convection at the bottom surface of the LED module, the total heat dissipation rate Q_h, based on Newton's law of cooling, is expressed as follows

$$Q_{\text{h}} = h_{\text{equ}}A(\overline{T}_L - T_a) \tag{25}$$

where A is the area of the heat sink's bottom surface, $(\pi/4)D_3^2$. Reconstructing (25), h_{equ} can be obtained and it is given by

$$h_{\text{equ}} = \frac{Q_{\text{h}}}{A(\overline{T}_L - T_a)} \tag{26}$$

According to (25), h_{equ} can be found if $\overline{T}_L$ is known. Since the area of the bottom surface A is very small, the temperature is distributed well at this surface. As a result, the temperatures of certain points on the surface can be considered as $\overline{T}_L$, and they will be obtained by simple experimental measurements.

There are many ways to measure $\overline{T}_L$. In this paper, a simple measurement method using a K-type thermocouple with diameter 0.3 mm is used to measure the temperature below the LED module, which was attached on a heat sink shown in Fig. 5 at room temperature of 22°C. For other applications, the fin heat sink can also be replaced by other heat sinks such as microchannels, thermoelectric coolers and so on. However, the method for measuring the temperature is the same. As the LED module is located on the heat sink shown in Fig. 5, a thermocouple should be located at the joint surfaces between the LED and heat sink. However, directly attaching a thermocouple between the LED module and the heat sink will increase the gap between the two components. Contact thermal resistance at the joint surface will increase

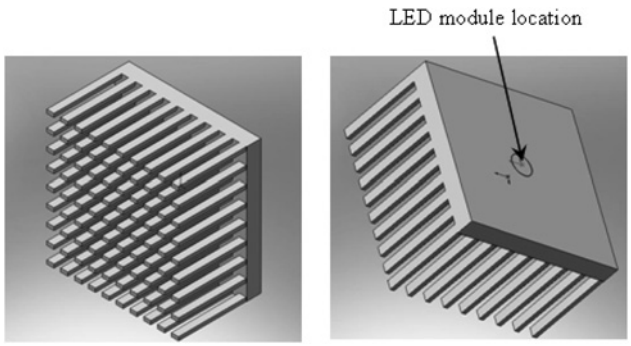

Fig. 5 *Application example: LED module attached with fin heat sink*

and cause unfavourable heat transfer. To solve the problem, thermal interface grease is pasted in the gap and a thermocouple is attached. It is nearly the same situation as the real case in which thermal interface grease is pasted between the LED module and the heat sink.

To calculate the heat generation rate exactly, the optical power should be excluded. Thus, the heat generation rate of an LED module is given by

$$Q_h = Q - Q_l \tag{27}$$

where Q is LED input power and Q_l is optical power of the LED. Both of those parameters can be easily measured by a spectrometer and its accessorial equipments.

In most LED products, many LED modules are arranged together on a heat sink. For those cases, the equivalent heat dissipation coefficient at each module's bottom surface can also be determined by measurement experiments of all the parameters needed in (26) and (27) for each module.

4 Results and discussion

4.1 Parameters and methods

To validate the proposed method, an LED module was selected for analysis using both the presented method and simulation. The dimensions and thermal parameters of the LED module are listed in Table 1. Thermal conductivity of TIM varied in the range of 2.45–50 W/(m K), for analysing its effect on the thermal characterisation of the LED module, whereas the other thermal parameters such as the boundary conditions and the dimensions remained the same. The results obtained by the thermal model and simulation were compared and analysed.

$\overline{T}_L$ was measured by the experiments mentioned in the last section and the result is 41 °C when the ambient temperature is 22 °C. According to the parameters and (25) and (26), the equivalent heat transfer coefficient can be found, and it is 1984 W/(m^2 K).

Table 1 Dimensions and thermal parameters of the LED module

Component	Parameter	Symbols	Value
LED chip	length, mm	–	0.96
	width, mm	–	0.96
	thickness, mm	–	0.08
	thermal conductivity, W/(m K)	–	40
	LED input power, W	Q	1.1804
	light radiation power, W	Q_l	0.1252
	heat generation rate, W	Q_h	1.0552
TIM	length, mm	a	0.96
	width, mm	b	0.96
	thickness, mm	t_{TIM}	0.05
aluminium stage	length, mm	c	1.45
	width, mm	d	1.45
	thickness, mm	t_{alu}	0.24
	thermal conductivity, W/(m K)	k_{alu}	236
copper heat sink	diameter of disc 1	D_1	2.91
	diameter of disc 2	D_2	6.52
	diameter of disc 3	D_3	5.97
	thickness of disc 1	t_1	1.74
	thickness of disc 2	t_2	0.44
	thickness of disc 3	t_3	0.37
	thermal conductivity, W/(m K)	k_{cop}	393

Simulations were done by software COMSOL. To provide a credible reference, the whole LED module was simulated. Considering symmetry of the module, only a quarter was simulated. The simulated structure is illustrated in Fig. 6. Thermal conductivities of PC lens and silicone were given as 0.16 and 1.8 W/(m K), respectively. All other surfaces except the bottom surface were loaded on a heat transfer coefficient of 5 W/(m^2 K) to simulate natural convection from these surfaces. h_{equ}, as it is 1984 W/(m^2 K), was given at the bottom surface. A tetrahedron mesh was applied to mesh the structure. Maximum element size of the TIM layer was set as 0.02 mm, whereas others were set by default value.

4.2 Results comparison and discussion

Fig. 7 shows the temperature distribution of the LED module, in which TIM's thermal conductivity is 2.45 W/(m K). Here, all temperatures on the module axis were treated as the mean temperatures of those surfaces. Based on the temperature distribution obtained by simulation, R_{TIM}, R_{alu}, R_{cop} and θ were calculated by the following equations

$$R_{TIM} = \frac{T_{c-s} - T_{s-a}}{Q_h} \tag{28}$$

$$R_{alu} = \frac{T_{s-a} - T_{a-c}}{Q_h} \tag{29}$$

$$R_{cop} = \frac{T_{a-c} - T_{c-b}}{Q_h} \tag{30}$$

$$\theta = T_{c-s} - T_{c-b} \tag{31}$$

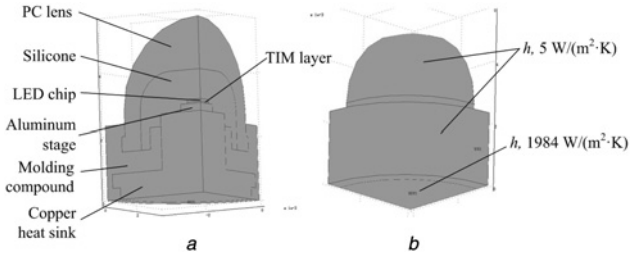

Fig. 6 *Simulation structure and boundary conditions*

a Simulation structure
b Boundary conditions

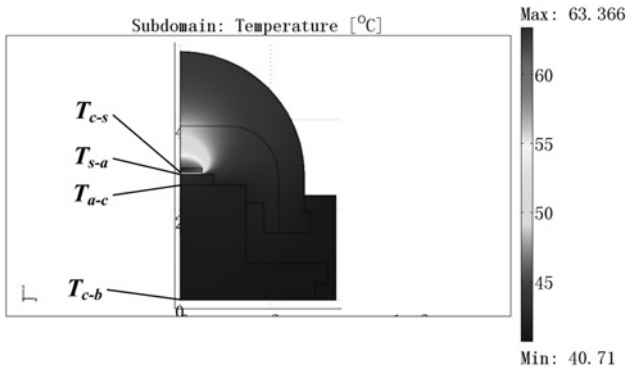

Fig. 7 *Temperature distribution of LED module with TIM (2.45 W/(m K)*

doi: 10.1049/iet-opt.2011.0004

Table 2 Results obtained by thermal model (*T*) and simulation (*S*)

Thermal conductivity of TIM, W/(m K)	R_{TIM}, °C/W		R_{alu}, °C/W		R_{cop}, °C/W		R_{total}, °C/W		θ, °C	
	T	*S*	*T*	*S*	*T*	*S*	*T*	*S*	*T*	*S*
2.45	22.144	18.205	0.652	0.758	1.378	1.223	24.174	20.186	25.509	21.300
5	10.851	9.856	0.652	0.843	1.378	1.26	12.881	11.96	13.592	12.620
10	5.425	5.127	0.652	0.881	1.378	1.289	7.455	7.2972	7.867	7.700
20	2.713	2.6061	0.652	0.891	1.378	1.298	4.743	4.7953	5.004	5.060
30	1.808	1.7343	0.652	0.9	1.378	1.298	3.838	3.9329	4.050	4.150
40	1.356	1.3078	0.652	0.891	1.378	1.308	3.386	3.5064	3.573	3.700
50	1.085	1.0425	0.652	0.891	1.378	1.308	3.115	3.2411	3.287	3.420

where T_{c-s} is the temperature of the intersection point of the axis with the top surface of TIM, T_{s-a} is the temperature of the intersection point of the axis with the bottom surface of the TIM or the top surface of the aluminium stage, T_{a-c} is the temperature of the intersection point of the axis and the bottom surface of the aluminium stage or the top surface of the copper heat sink, T_{c-b} is the temperature of the intersection point of the axis and bottom surface of the LED module.

Thermal conductivity of the TIM varied from 2.45 to 50 W/(m K). The results obtained by the thermal model and simulations are compared in Table 2. Here, '*T*' means analytical results, '*S*' means simulation results.

In Table 2, it is clear that R_{total} and the junction temperature difference θ calculated by the thermal model are close to the ones obtained by simulation. This demonstrates that the thermal model is valid for junction temperature prediction in engineering applications.

From Table 2, it can be seen that the thermal resistance of the TIM comprises the majority of the total thermal resistance of the LED module. As a result, reducing this portion of thermal resistance will greatly improve thermal characterisation of the LED module. Table 3 shows junction temperatures obtained by the thermal model and simulation with different TIM layers. Fig. 8 is the curve plot based on the data in Table 3. As shown in Fig. 8, the junction temperature of the LED module drops significantly with an increase in the thermal conductivity of TIM. Therefore thermal interface materials with high thermal conductivity should be used in the LED module to reduce thermal resistance of LED module.

It should be noted that the ideas behind the thermal model can be applied for other LED module structures. For instance, in many LED modules, the LED chip may be bonded directly to the small heat slug using eutectic soldering. For these modules, the structure is a little different from the one in the thermal model presented here. However, the present thermal model can be adjusted to analyse its thermal characterisation by substituting the present TIM with eutectic soldering and deleting the aluminium stage. In addition, as mentioned earlier, the present method to predict junction temperatures can also be used in LED module arrays and other application products such as LED street lamps by applying the equivalent heat transfer coefficient. Therefore the present method can be commonly used for predicting junction temperature in engineering applications.

Table 3 Junction temperatures of LED module obtained by analytical model and simulation

Thermal conductivity of TIM, W/(m K)	Junction temperature, °C, '*T*'	Junction temperature, °C, '*S*'
2.45	66.509	63.389
5	54.592	54.833
10	48.867	49.975
20	46.004	47.356
30	45.050	46.457
40	44.573	46.002
50	44.287	45.727

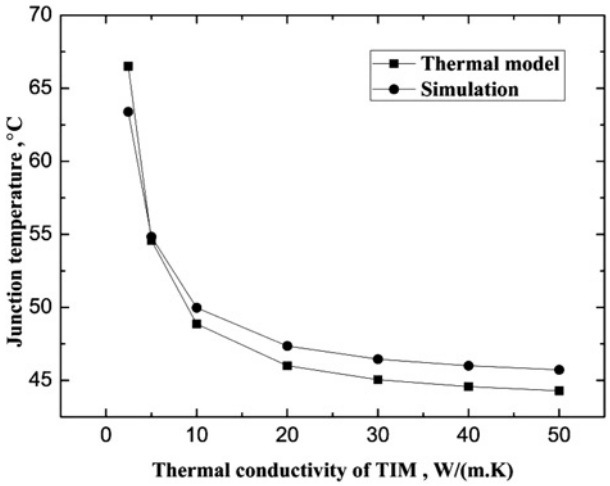

Fig. 8 *Variation of junction temperature with thermal conductivities of TIM*

5 Summary and conclusions

A thermal model to predict the junction temperature of a typical LED packaging module was presented. The proposed thermal model and simulation were used to analyse thermal characterisation of an LED module with varied thermal parameters. Comparison of the results obtained by simulation and the thermal model shows that the proposed method is an effective engineering method for predicting the junction temperature of a typical LED module. According to the thermal model and the analysis of an LED module, it was also found that the bonding material and processes between the chip and the small heat slug in LED packaging have an obvious effect on junction temperatures. High thermal conductivity materials or a better structure should be used in LED packaging for good thermal management.

6 Acknowledgments

The authors acknowledge the financial support in part from 973 Project of the Ministry of Science and Technology of

China (no. 2011CB013105) and in part by National 863 project of the Ministry of Science and Technology of China (no. 2011AA03A109).

7 References

1 Chen, N.C., Wang, Y.N., Tseng, C.Y., Yang, Y.K.: 'Determination of junction temperature in AlGaInP/GaAs light emitting diodes by self-excited photoluminescence signal', *Appl. Phys. Lett.*, 2006, **89**, (10), pp. 101114–101114-3

2 Kirkup, L., Kalceff, W., McCredie, G.: 'System for measuring the junction temperature of a light emitting diode immersed in liquid nitrogen', *Rev. Sci. Instrum.*, 2006, **77**, (4), pp. 046107–046107-3

3 Gu, Y.M., Nadarajah, N.: 'A Non-contact method for determining junction temperature of phosphor-converted white LEDs', *SPIE Proc.*, 2004, **5187**, pp. 107–114

4 Chen, Q., Luo, X.B., Zhou, S.J., Liu, S.: 'Dynamic junction temperature measurement for high power light emitting diodes', *Rev. Sci. Instrum.*, 2011, **82**, p. 084904

5 Luo, X.B., Cheng, T., Xiong, W., Gan, Z.Y., Liu, S.: 'Thermal analysis of an 80 W light-emitting diode street lamp', *IET Optoelectron.*, 2007, **1**, (5), pp. 191–196

6 Bar-Cohen, A., Elperin, T., Eliasi, R.: 'θjc Characterization of chip packages – justification, limitations, and future', *IEEE Trans. Compon. Hybrids Manuf. Technol.*, 1989, **12**, (4), pp. 724–731

7 Rosten, H.I., Lasance, C.J.M., Parry, J.D.: 'The world of thermal characterization according to DELPHI-part I: Background to DELPHI', *IEEE Trans. Compon. Packag. Manuf. Technol. A*, 1997, **20**, (4), pp. 384–391

8 Lasance, C.J.M., Parry, J.D., Rosten, H.I.: 'The world of thermal characterization according to DELPHI-Part II: Experimental and numerical methods', *IEEE Trans. Compon. Packag. Manufact. Technol. A*, 1997, **20**, (4), pp. 392–398

9 Lasance, C.J.M., Vinke, H., Rosten, H., Weiner, K.L.: 'A novel approach for the thermal characterization of electronic parts'. Proc. 11th IEEE Proc SEMI-THERM Conf., San Jose, CA, USA, 1995, pp. 1–9

10 Kennedy, D.P.: 'Spreading resistance in cylindrical semiconductor devices', *J. Appl. Phys.*, 1960, **31**, (8), pp. 1490–1497

11 Kadambi, V., Abuaf, N.: 'An analytical of thermal response for power chip packages', *IEEE Trans. Electron. Devices*, 1985, **ED-32**, (6), pp. 1024–1033

12 Krane, M.J.H.: 'Constriction resistance in rectangular bodies', *ASME J. Electron. Packag.*, 1991, **113**, pp. 392–396

13 Muzychka, Y.S., Stevanovic, M., Yovanovich, M.M.: 'Spreading thermal resistance in Compound Annular Sectors', *J. Thermophys. Heat Transf.*, 2001, **15**, (3), pp. 354–359

14 Muzychka, Y.S., Yovanovich, M.M., Culham, J.R.: 'Application of spreading thermal resistance in compound and orthotropic systems'. Proc. 39th AIAA Aerospace Sciences Meeting and Exhibit, Reno, NV, USA, 2001, AIAA 01-0366

15 Muzychka, Y.S., Yovanovich, M.M., Culham, J.R.: 'Spreading thermal resistances in rectangular flux channels part I – geometric equivalences'. Proc. 36th AIAA Thermophysics Conf., Orlando, Florida, USA, 2003, AIAA 2003-4187

16 Luo, X.B., Xiong, W., Cheng, T., Liu, S.: 'Temperature estimation of high power light emitting diode street lamp by a multi-chip analytical solution', *IET Optoeletron.*, 2009, **3**, (5), pp. 225–232

17 Cheng, T., Luo, X.B., Huang, S.Y., Liu, S.: 'Thermal analysis and optimization of multiple LED packaging based on a general analytical solution', *Int. J. Therm. Sci.*, 2010, **49**, pp. 196–201

18 Luo, X.B., Mao, Z.M., Liu, S.: 'Analytical thermal resistances model for eccentric heat source on rectangular plate with convective cooling at upper and lower surfaces', *Int. J. Therm. Sci.*, 2011, **50**, pp. 2198–2204

19 Luo, X.B., Mao, Z.M., Liu, J., Liu, S.: 'An analytical thermal resistance model for calculating mean die temperature of a typical BGA packaging', *Thermochim. Acta*, 2011, **512**, pp. 208–216

doi: 10.1049/iet-opt.2011.0004